

Mathematical modeling of separation behaviour of a spiral for washing high ash coal

**S.K.Das, K.M.Godiwalla, Lopamudra Panda, K.K.Bhattacharya, Ratnakar Singh
and S.P.Mehrotra**

**National Metallurgical Laboratory
(Council of Scientific & Industrial Research)
Jamshedpur 831007, India**

E-mail : skd@nmlindia.org

ABSTRACT

Sustained Coal R&D activity has been crucial to the many successful clean coal technology developments that have been achieved globally. The aim has been to enhance the competitiveness of coal by providing technical and environmental improvements whilst at the same time reducing capital and operating costs. In coal preparation, simpler lower cost alternatives to froth flotation, such as the coal dense medium separator and spiral separators, have been adapted for cleaning of fine coal. A mathematical model has been developed to characterize the separation behavior of a typical high ash coal in a spiral. The modeling framework consists of parametric representation of geometry of the spiral and its trough, particulate flow along the helical path and principal forces acting on a particle during its motion. The elements have been combined seamlessly by assuming that the particles eventually attain dynamic equilibrium in the forward longitudinal direction and static equilibrium in the transverse direction. The resulting force function provides a spectrum of the particles' radial location on the trough according to their size and relative specific gravity. The model predicts relative specific gravity distribution and particle size as a function of equilibrium radial position. Sensitivities of radial equilibrium distribution of particle size and relative specific gravity with respect to mean flow depth have also been investigated. Simulation results are encouraging and validated with the published data. The model provides an analytical tool for better understanding of the separation behavior of particles in a coal-washing spiral.

Key words: Spiral separator, coal washing, fluid flow, equilibrium force balance, relative specific gravity, particle size

1.INTRODUCTION

Cleaner production and eco-efficiency are complimentary strategies, essentially dealing with the use of minerals, materials, energy and water. Both are generic improvement and innovation strategies with well established track records in many industries, in particular in processing and extraction of minerals and metals.

Coal plays a central role in the economy of the country. It has accounted for 75 % of annual energy use over the years. Whilst it is cheap and plentiful, the environmental and health effects of usage of coal are becoming more and more severe as the economy continues to grow at a rapid rate. There is an increasing need to find ways of limiting pollution of the air and water through the use of cleaner technologies and more efficient processes. Clean coal technologies have the potential to reduce emissions of the gases, in the user industries which cause urban smog, high level of particulate emission and acid rain. Further, power plants that use fossil fuels to generate electricity currently face a myriad of environmental regulations intended to restrict releases to the air, water and land. The regulatory measures are stringent for controlling NO_x , SO_2 and fly ash contents in the emissions.

Gravity concentration of minerals has traditionally been recognized as a low cost and environmentally friendly process for the separation of minerals. In recent years a number of new process technologies have emerged allowing ever-finer materials to be successfully processed. Spirals separators are simple, low energy consuming devices that separate minerals based on their respective densities and have proven to be metallurgically efficient and cost effective since their widespread commercial introduction more than 50 years ago. Most bituminous coal is cleaned by conventional methods that have been slowly improved over the years and truly few new beneficiation technologies have made any significant inroads in the past 10-20 years. This is particularly true of

processes for cleaning the coarse and intermediate sizes of coal (down to about 0.5 mm) where highly efficient dense-media processes predominate. For particle sizes in the range of about 1.0 mm down to about 0.1 mm that straddle the lower end of the intermediate size and the upper end of the fine size, recent improvements in the design of spiral concentrators and the re-engineering of spiral circuits have resulted in improved performance and a resurgence usage of the spiral in washing high ash coal for power plant and blast-furnace applications.

The generic geometry of spiral concentrators consists of an open trough that spirals vertically downwards in helix configuration about a central axis. Employed in the fine coal, a slurry mix of fine particles is fed to the top of the spiral and, as it gravitates downwards, particles are segregated radially across the trough by the centrifugal force. Separation occurs as light suspended particles travel to the outer trough regions whilst heavy particles settle and tend to move inwards towards the central column. Historically, evolution of the design has been almost exclusively based on empirical development of the appropriate geometry. Fig.1 shows a sectional view of spiral trough flow.

In recent years, because of the industrial demand, there has been an upsurge of interest in usage of spirals primarily for processing of coal in the intermediate size range of 0.01mm to 3 mm [1-4]. These coal particles are neither large enough for heavy media separation nor small enough for froth floatation. Several improvements in coal spiral performance have been seen over the years. Recent studies have concentrated on optimizing the number of turns required on a spiral. This effort is an attempt to standardize the required number of turns needed on a spiral for different minerals. As recent as the 1960's, Australian coal spirals had as few as two full turns, while modern spirals can employ as many as seven turns to achieve the required separation [5-6].

Studies have also shown that the feed rate, especially the total volumetric flow, introduced onto a spiral can greatly affect its performance. It has been stated in the investigation by Holland-Batt [6] that the total mass feed rate is among one of the most important factors for determining coal spiral capacity.

Their work indicates that, for any feed pulp density, there exists an optimum feed rate. Further studies [7] show that spiral performance that is considerably affected by slurry density, and further indicates that a more dominant control of spiral performance has been observed when combining slurry density with the solid flow rate (i.e. volumetric feed rate). As volumetric feed rate is increased, an increasing amount of entrained material will report to the outer wall and effectively reduce efficiency.

Current theoretical understanding of coal-processing spirals is mostly empirical. Until recently, modeling and analysis of spiral performance have met with only limited success, since their introduction in mineral processing operations [5-8]. There exists a genuine need for improving the efficiency of spirals. It is well known that sharpness of separation, size, density, range of feed particles (coal) and throughput capacity of spirals have a direct bearing on the efficiency and productivity of the coal cleaning.

A mathematical model has been developed for coal processing spirals to study the sensitivity of the operating parameters on the separation behavior of the particle during its descent along the helical path. It is expected that the model can reasonably mimic the behavior of the particle during its motion along the spiral with a reasonable degree of realism. The model comprises of three important aspects of spiral separator which has been incorporated to formulate a reasonably hybrid methodology using first principle based approach coupled with semi-empirical correlations. This comprises of modeling of spiral geometry, fluid flow based on sediment transport concept and force balance on coal particles moving down the spiral based on conservation principle. This model has been used to analyze the separation characteristics of a typical high ash content coal (Patherdih , Jharkhand) .

2.MATHEMATICAL MODEL

The mathematical model comprises of the sub-models addressing the aforesaid components. These are seamlessly integrated to characterize the separation characteristics of the particles in terms of distribution of relative specific gravity and particle size along the radial equilibrium position. Mean flow

depth sensitivity has been studied with respect to relative specific gravity variation at various equilibrium position.

2.1. Sub-model for spiral geometry.

It is evident that the performance of coal processing spiral would depend critically on design parameters such as diameter, height, number of turns, pitch and slope as well as the shape of the trough and its dimension. Geometrically, the channel may be visualized as comprising of an infinitely large number of axially adjacent non- intersecting helical curves.

The parametric equations of a helix in Cartesian coordinate system can be represented in the following manner [6-7, 15];

$$x = r \sin[\eta] \quad (1)$$

$$y = r \cos[\eta]; 0 \leq \eta \leq N\pi \quad (2)$$

$$z = \frac{U}{2 * \pi} \eta; 0 \leq z \leq H \quad (3)$$

where, N is twice the number of turn, H is spiral height and r is the radial distance from the central line. Here η is the parameter used for parametric representation of the co-ordinates in eqns.(1)-(3). Figure 2 shows the geometric parameters of the spiral. From these equations the longitudinal tangential slope, S at any point on the trough may be derived by the following equation;

$$S = \tan[\alpha] = \frac{U}{2\pi r} \quad (4)$$

Where U is the pitch of the spiral, and α is the slope angle. The local slope of the channel in the radial or transverse direction may be determined by the following equation;

$$\tan[\theta] = \frac{c_y}{r_o - r_i} \tan \arcsin \left[\frac{r - r_i}{r_o - r_i} \right] \quad (5)$$

Where θ is the local slope angle in the transverse direction, c_y is the maximum depth of the trough and r_i and r_o are respectively inner and outer radii of the trough from the central line /symmetry axis of the spiral and, $r_i \leq r \leq r_o$.

2.2. Semi-empirical modeling of fluid flow

The spirals exhibit one of the most complex flow regimes among gravity separators used in mineral /coal processing operations. Spiral concentrator flows possess a free-surface, have shallow depths of <10 mm typically, and display laminar to increasingly turbulent behavior radially outwards with velocities reaching 3 m/s [3-6].

Current understanding of the mechanism of separation on spiral separators involves primary and secondary flow patterns [6]. These flow patterns allow for dilation of the particle bed and provide opportunities for separating mechanisms to occur. The primary flow is that of the slurry descending the incline of the trough. Secondary flow occurs radially across the trough. The upper, more fluid layers move away from the center while the lower, more concentrated layers (especially where particles are in contact with the solid surface) move towards the centre. Stratification occurs and the secondary flow causes shearing of the strata, resulting in bands of higher density particles reporting to the inner region of the trough. A secondary circulation current in a plane perpendicular to the mainstream flow direction, induced by the spiral curvature and resultant centrifugal force, travels outwards near the free-surface and back inwards towards the central column near the trough base.

To model this flow, it is imperative to consider the fluid phase to be Newtonian, and possess constant physical properties. The fluid dynamics is essentially represented by the Reynolds-averaged turbulent Navier±Stokes equations. For a coal processing spiral, the steady-state equations for the conservation of mass and momentum in generalized curvilinear form, are respectively given by:

$$\frac{\partial \rho u_i}{\partial x_i} = 0 \quad (6)$$

$$\frac{\partial}{\partial x_i} (\rho u_i u_j) = -\frac{\partial P}{\partial x_i} + \rho g_i + \frac{\partial}{\partial x_i} \left[\mu_{eff} \left(\frac{\partial u_i}{\partial x_j} + \frac{\partial u_j}{\partial x_i} \right) \right] \quad (7)$$

where ρ is the fluid density, μ_{eff} the effective (molecular μ plus turbulent μ_t) viscosity, P the static pressure, and u_{ij} , and g_i the mean velocity and gravitational acceleration, respectively. To consider the effects of turbulence, appropriate turbulence model, such as (K- ϵ) model or RNG based (K- ϵ) model can be applied in conjunction with Navier-Stokes equations,(6) and(7). Computational Fluid Dynamic (CFD) analysis of the spiral particulate flow behavior and particle dynamics is a formidable task which requires commercial CFD software for flow simulation and mapping. The fundamental approach through the solutions of Navier-Stokes equations with appropriate boundary conditions has not yet been reported in the literature for comprehensive two-phase particulate flow prevailing in the spiral. Without the multiphase analysis, the computational results are unlikely to be commensurate with the enormous computational times required.

2.2.1 Power law treatment of the flow

A more practical approach for flow modeling in spiral relies on velocity profiles as predicted by assuming appropriate flow regimes [8-11]. The action of centrifugal force on water as it flows down in a spiral channel has two important consequences. First the water level at the outer concave wall of the trough exceeds that at the inner convex is generated in the form of a vertically flattened helical spiral that moves forward in a corkscrew fashion. The angles that the inward and outward-bound flows make with the mean axial flow vary with depth and radial distance. Holland-Batt[3] and Holthman[12] have reported measurements of these angles obtained in pure water which are typically applicable analysis of heavily loaded slurries. An expression widely quoted in hydrology literature [14-15] for determining the mean deviation angle, δ .

$$\tan[\delta] = 11 \frac{h_f}{r} \quad (8)$$

Where, δ is the mean deviation angle, h_f is the depth of the flow and r is the radial equilibrium position. In this analysis an averaging approach [12-13] has been employed as a matter of practical expediency and with no pretensions for describing the flow either precisely or in detail. Flow of fluids and sediments in

open channels are commonly described by a plethora of power laws whose general form is:

$$\langle V \rangle = \gamma R^a S^b \quad (9)$$

Where $\langle V \rangle$ is the mean flow velocity, R is hydraulic radius and γ is a composite resistance coefficient. The exponents 'a' and 'b' depend on the nature of flow such as laminar, Manning laminar, Lacey rough channel, Blasius turbulent, Blagnold suspension, transitional or mixed type or a combination thereof [9]. The transitional or mixed flow equation has been employed to describe the flow behaviour [14-15]. The mean flow velocities computed with these equations are comparable with the measured data, even though the computed flow depths turn out to be greater than reported values. The power law for transitional or mixed flow is described by the following semi-empirical equation [12-15];

$$\langle V \rangle = \frac{26.4}{d_p^{1/6}} R \sqrt{S} \quad (10)$$

Where d_p is a percentile size in the solid feed. Another expression for the mean velocity is:

$$\langle V \rangle = \frac{Q}{A} \quad (11)$$

Where, Q is the volumetric feed rate and A is the cross-sectional area of flow. Measurements on water only spiral by Holtham [12-13] demonstrated that the depth of flow increases from about 1mm at the inner end of the spiral to 8-10mm or more depending upon the feed rate and spiral type near the outer end just before dropping to zero at the waiting limit.

The tangential slope, S in equation (10) is re-designated as S_m , which represents the channel tangential slope at the mid point. This has been substituted along with appropriate expressions for R and A in terms of the trough geometry and mean flow depth, h_m and finally $\langle V \rangle$ has been eliminated between equations (10) and (11) and the following equations for calculating total flow rate has been arrived at:

$$Q = \frac{3.3\pi^{1.5}}{2d_p^{1/6}} \sqrt{\frac{U}{c_x} \frac{[c_x c_y - (c_x - h_m)(c_y - h_m)]^2}{\int_0^{\pi/2} \sqrt{(x'^2 + y'^2)} d\eta + h_m}} \quad (12)$$

Where x' and y' are derivatives of x and y with respect to η i.e $x' = dx/d\eta$, $y' = dy/d\eta$ and $c_x = r_o - r_i$ is the radial width of the trough. Equation(12) can be solved for mean flow depth which will be required for implementation of the force equilibrium model.

The integral in eqn.(12) can be evaluated and substitution of the same gives the final expression of the volumetric feed rate(Q) as:

$$\int_0^{\pi/2} \sqrt{(x'^2 + y'^2)} d\eta = r\pi/2 \quad (13)$$

$$Q = \frac{3.3\pi^{1.5}}{2d_p^{1/6}} \sqrt{\frac{U}{c_x} \frac{[c_x c_y - (c_x - h_m)(c_y - h_m)]^2}{r\pi/2 + h_m}} \quad (14)$$

The governing equation for calculation of mean flow depth, h_m , has been derived using eqn.(14) and given as:

$$h_m^4 - 2(c_x + c_y)h_m^3 + (c_x + c_y)^2 h_m^2 - \frac{Q(2d_p^{1/6})}{3.3\pi^{1.5} (\frac{U}{c_x})^{1/2}} h_m - \frac{Q(2d_p^{1/6})}{3.3\pi^{1.5} (\frac{U}{c_x})^{1/2}} \pi r_m = 0 \quad (15)$$

Where r_m is the mean radial position from the central line i.e, $(r_o + r_i)/2$.

2.3. Force equilibrium sub model

The forces acting on the particle during it's motion in the spiral separator are critical to dictate the dynamics of the particle and performance of the system. It is not easy to identify and quantify most of these forces precisely. In general, only rough estimates of the five principal forces involved, namely gravity, centrifugal, hydrodynamic drag, lift and friction forces can be made [14-15]. In addition, "Bagnold effect" arises at high pulp densities of the feed . It is attributed to the existence of velocity distribution along the depth of flowing film, giving rise

to a distribution of shear rate along the flow depth . As a result the Bagnold forces, acting on particles located at different depths and having different sizes and densities, will be different in magnitude for each particle in the pulp[15].

In particulate flow system, fluid driven particles move by one or more of the following modes: sliding, rolling, saltation. How ever, trajectory simulation of particles in a particulate flow system is a arduous task and such work has not yet reported in the literature. Under steady state condition, it is presumed that, particles are in dynamic equilibrium in the longitudinal direction and in static equilibrium in the transverse direction. The static equilibrium analysis provides an understanding of segregation of particles according to their density and size during their descent along the helical path of the spiral. Neglecting the "Bagnold effect", the longitudinal component of all forces (F_L) acting on a particle in steady motion is [14-15] :

$$F_L = F_g \sin[\theta] \sin[\alpha] - F_c \cos[\theta] \sin[\alpha] + F_d \cos[\delta] - F_N \tan[\phi] = 0 \quad (16)$$

Where F_g is the gravity force, F_c is the centrifugal force, F_d is the drag force and F_N is the normal component of all forces. The normal component of the force is given as:

$$F_N = F_g \cos[\theta] + F_c \sin[\theta] - F_l \quad (17)$$

where , F_l is the lift force acting on the particle. The transverse component of forces acting on a stationary particle is:

$$F_T = F_c \cos[\theta] \cos[\alpha] + F_d \sin[\delta] - F_g \sin[\theta] \cos[\alpha] = 0 \quad (18)$$

Combining these expressions with the elimination of centrifugal force term yields a force function given bellow:

$$\frac{F_l \tan[\phi] + F_d \cos[\delta] - F_g (\tan[\phi] \cos[\theta] - \sin[\alpha] \sin[\theta])}{\cos[\theta] \sin[\alpha] + \tan[\phi] \sin[\theta]} = \sec[\alpha] \sec[\theta] x \quad (19)$$

$$(F_d \sin[\delta] - F_g \cos[\alpha] \sin[\theta])$$

Substitution for gravity, drag and lift forces results in the following equation

$$\begin{aligned} & \frac{\rho h S}{4\sqrt{1+S^2}} \left[\frac{k_1 \tan[\phi] + \cos[\delta] + \sin[\delta] \tan[\alpha] + \tan[\phi] \sec[\alpha] \sin[\delta] \tan[\theta]}{\cos[\theta] \sin[\alpha] + \tan[\phi] \sin[\theta]} \right] \\ & = \frac{d_p g \tan[\phi] (\sigma - \rho)}{6} \left[\frac{\cos[\theta] + \sin[\theta] \tan[\theta]}{\cos[\theta] \sin[\alpha] + \tan[\phi] \sin[\theta]} \right] \end{aligned} \quad (20)$$

Substitution of S and angles α, θ, δ as given in equations (4),(5),(6) respectively and h_m from equation (14) result in the following expression :

$$\begin{aligned} \frac{\sigma - \rho}{\rho} &= \frac{U h_m 6 \cos(\tan^{-1}(\frac{c_y}{r_0 - r_i} \tan \arcsin[\frac{r - r_i}{r_0 - r_i}]))}{d_p g \tan \phi 4 \sqrt{(U)^2 + (2\pi r)^2}} [k_1 \tan \phi + \cos(\tan^{-1}(11 \frac{h_m}{r})) + \\ & (\sin(\tan^{-1}(11 \frac{h_m}{r}))) (\frac{U}{2\pi r}) + \tan \phi \sec(\tan^{-1}(\frac{U}{2\pi r})) \sin(\tan^{-1}(11 \frac{h_m}{r})) (\frac{c_y}{r_0 - r_i} \tan \arcsin[\frac{r - r_i}{r_0 - r_i}])] \end{aligned} \quad (21)$$

and, the expression for particle size is,

$$\begin{aligned} d_p &= \frac{\rho U h_m 6 \cos(\tan^{-1}(\frac{c_y}{r_0 - r_i} \tan \arcsin[\frac{r - r_i}{r_0 - r_i}]))}{(\sigma - \rho) g \tan \phi 4 \sqrt{(U)^2 + (2\pi r)^2}} [k_1 \tan \phi + \cos(\tan^{-1}(11 \frac{h}{r})) + \\ & (\sin(\tan^{-1}(11 \frac{h}{r}))) (\frac{U}{2\pi r}) + \tan \phi \sec(\tan^{-1}(\frac{U}{2\pi r})) \sin(\tan^{-1}(11 \frac{h}{r})) (\frac{c_y}{r_0 - r_i} \tan \arcsin[\frac{r - r_i}{r_0 - r_i}])] \end{aligned} \quad (22)$$

The relative specific gravity is defined as the ratio of difference between particle and water density and density of water i.e $(\sigma - \rho)/\rho$. This parameter is indicative of the relative specific gravity variation during classification operation. Equation (21) has been employed to compute the relative specific gravity as a function of equilibrium position for various particle sizes. Similarly equation (22) has been employed to compute the particle size as a function of various equilibrium positions for different relative specific gravity. The best estimates of k_1 and ϕ

available in the literature [14-15], have been incorporated in the model for prediction of relative specific gravity and particle size for a typical spiral data.

2.4.Numerical Implementation

In order to solve the governing model equations (15), (21) and (22) by an iterative scheme; a **C++** code is developed to compute geometric parameters, flow parameters involving mean flow depth, distribution of relative specific gravity and particle size as a function of equilibrium position. The design data of a typical coal-washing spiral, located in the pilot plant of the laboratory(NML), has been used in this simulation. The data are given in Table-1.The volumetric feed rate (Q) is taken in the range of 0.3 to 0.6m³/hr . Patherdih (Jharkhand) coal fines are used for the washability studies.

TABLE-I

Design data of the coal-washing spiral (NML)

(i) Height (H)=2.5m	(ii) Pitch(U)=0.425m
(iii) Slope (S)=(tan α)=0.17	(iv) Outer Radius (r _o)=0.48m
(v) Inner Radius (r _i)=0.08m	(vi) Trough slope(tan θ)=0.2
(vii) Max. depth(c _y)=0.15m	(vii) Radial width(c _x)=0.4m

3.RESULTS AND DISCUSSION

Figures (3-5) show the distribution of relative specific gravity as a function of equilibrium radial position, (r_o-r_i) for different particle sizes, namely 1mm, 1.25mm, 1.5mm, 1.75mm and 2mm respectively. Sensitivity of distribution of relative specific gravity with respect to mean flow depth (h_m) has also been studied. Figures (3),(4)and(5) refer to mean flow depth 5mm, 4mm and 3mm respectively. In each of these figures distribution of relative specific gravity as a function of equilibrium position monotonically decreases with the increase in particle size. The negative slope of these curves, i.e the gradient of relative

specific gravity per unit radial distance $\frac{d}{dr} \left(\frac{\sigma - \rho}{\rho} \right)$, is a measure of the separation efficiency. This means, the lower the slope, the greater is the efficiency. Figures (6-8) show the distribution of particle sizes as a function of equilibrium radial position, $(r_o - r_i)$ for different relative specific gravity, namely 0.75, 1, 1.25 and 1.5 respectively. Sensitivity of distribution of particle size with respect to mean flow depth (h_m) has also been investigated.

As observed in actual spiral operation, as well as in this simulation results that lighter particles are segregated in the outer region while the heavier particles are concentrated in the inner region of the trough for all considered values of particle relative specific gravity. The present force equilibrium spiral model, even without tuning the adjustable parameters, yields reasonably realistic values for both particle-fluid relative specific gravity and particle size.

Figures (9-11) show the particle relative specific gravity variation as a function of mean flow depth at various equilibrium positions (100mm, 200mm, 300mm and 400mm) for different particle sizes, namely, 1mm, 1.5mm and 2mm respectively. It may be observed that for all radial equilibrium positions, the relative specific gravity between the particle and water decreases with increase in particle size as a function of mean flow depth. However relative specific gravity between the particle and water increases almost linearly with increase in mean flow depth irrespective of particle size. This is valid for all equilibrium radial positions as depicted in these figures.

The simulation results generated by this model have been verified with the literature [12-15]. The order of magnitude and characteristics of the equilibrium radial distribution of spiral process variables (relative specific gravity and particle size) are found in good agreement.

4.CONCLUSION

The model presented here incorporates three principal components of equilibrium force balance formulation. They are; spiral geometry, flow characterization and forces acting on the particle. This investigation has also vindicated that it is feasible to characterize the hydrodynamic behavior of an

industrial spiral (involving calculation of mean flow depth) using power law formalism of hydrology without resorting to the solution of the Navier-Stokes equation for the complex spiral geometry. The present model provides better understanding of the separation behavior of high ash coal based on its specific gravity distribution along the equilibrium position. Although the steady state attainment of the flow field is a debatable issue, nevertheless, the simulation results suggest that the force equilibrium methodology could provide a useful simulation framework provides a quantitative picture of the particle behavior and separation characteristics in an operating spiral. The semi-empirical approach for fluid dynamic analysis is justified by the need for developing a working hydrodynamic model for an operating spiral with a complex spectrum of flow regimes. Further refinement of the quantitative hydro-dynamical description of spiral, without intensive and time consuming computations still remains a challenging task. Future attempts will be made to calibrate the adjustable parameter with the plant data for implementation of the model. The results are encouraging to infer that the model presented here does have a predictive capability for analyzing separation characteristics of coal grades with varying ash content by a water only spiral. It is expected that the calibrated model will provide useful guidelines to optimize the operating parameters for improving washability performance of spiral in view of growing demand for usage of low ash coal in power plant and steel sectors to meet the environmental regulatory requirements.

REFERENCES

1. Chedgy, D.G., Placha, D.S. and Watters, L.A., "Spiral Concentrators for Fine Coal Processing, "PCMIA/SME Joint Meeting, Washington, PA, November 1-2, 1990.
2. Edward, D., Li, M., Davis, J. and Kruitschnitt, J., "Spiral Research: Technique Development and Use," Pittston Coal Management Co., Paper B2, 1998, pp. 100-119.
3. Holland-Batt, A.B., "Interpretation of Spiral and Sluice Tests," Trans. Instn. Mining and Metallurgy, 1990, Vol. 99, pp. C1-C20.

4. Holland-Batt, A.B., "A Study of the Potential for Improved Separation of Fine Particles by Use of Rotating Spirals," *Minerals Engineering*, 1992, Vol. 5, Nos. 10-12, pp. 1099-1112.
5. Holland-Batt, A.B., "The Effect of Feed Rate on the Performance of Coal Spirals," *Coal Preparation*, 1994, Vol. 14, pp. 199-222.
6. Holland-Batt, A.B., "The Dynamics of Sluice and Spiral Separations," *Minerals Engineering*, 1995, Vol. 8, No. 1/2, pp. 3-21.
7. Holland-Batt, A.B., "Gravity Separation: A Revitalized Technology," *Mining Engineering*, 1998, Vol. 50, No. 9, pp. 43-48.
8. MacNamara, L., Addison, F., Miles, N.J., Bethell, P. and Davies, P., "The Application of New Configurations of Coal Spirals," *Proceedings, 12th International Coal Preparation Conference and Exhibit*, Lexington, Kentucky, May 2-4, 1995.
9. MacNamara, L., Toney T.A., Moorhead, R.G., Miles, N.J., Bethell, P. and Everitt, B., "On Site Testing of the Compound Spiral," *Proceedings, 13th International Coal Preparation Conference and Exhibit*, Lexington, Kentucky, April 30-May 2, 1996.
10. Walsh, D.E. and Kelly, E.G., "An Investigation of the Performance of a Spiral Using Radioactive Gold Tracers," *Minerals and Metallurgical Processing*, 1992, Vol. 9, No. 3, pp.105-109
11. Weldon, W.S. and Mac Hunter, R.M.G., "Recent Advances in Coal Spiral Development," *SME Annual Meeting*, Denver, Colorado, Preprint No. 97-82, Feb. 24-27, 1997.
12. Kapur, P.C. and Meloy, T.P., "Spirals Observed," *Inter. J. Mineral Processing*, 1998, Vol.53, pp.15-28.

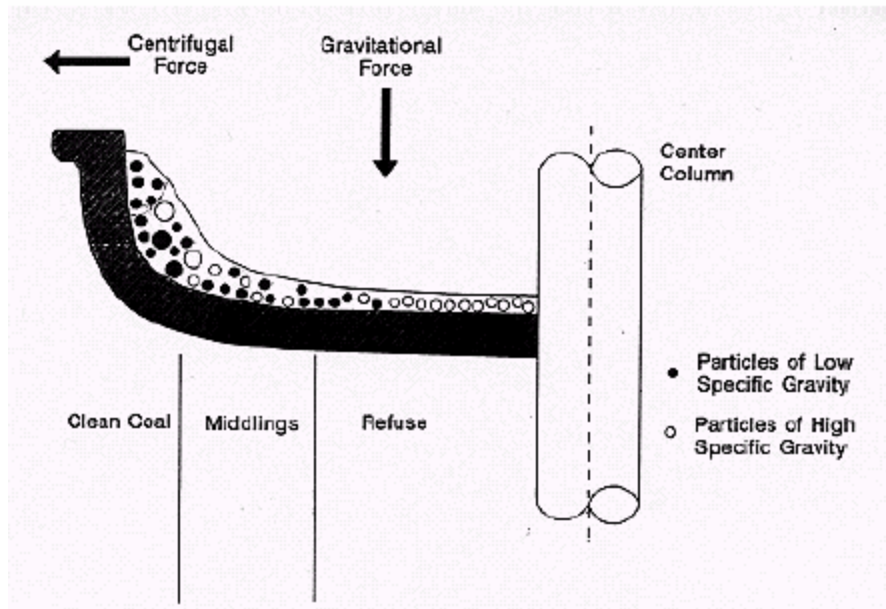


Fig1.A sectional view of the a spiral trough flow

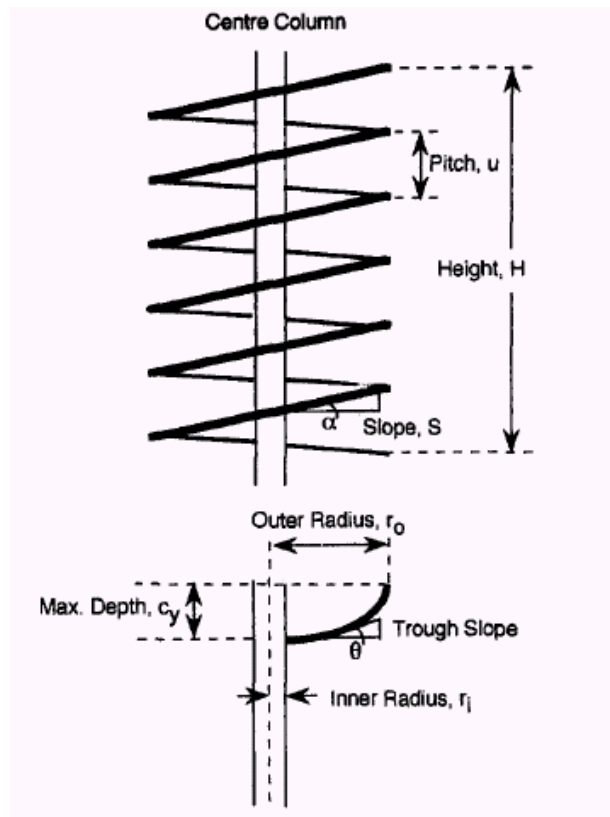


Fig.2 Geometric / design parameters of spiral [15]

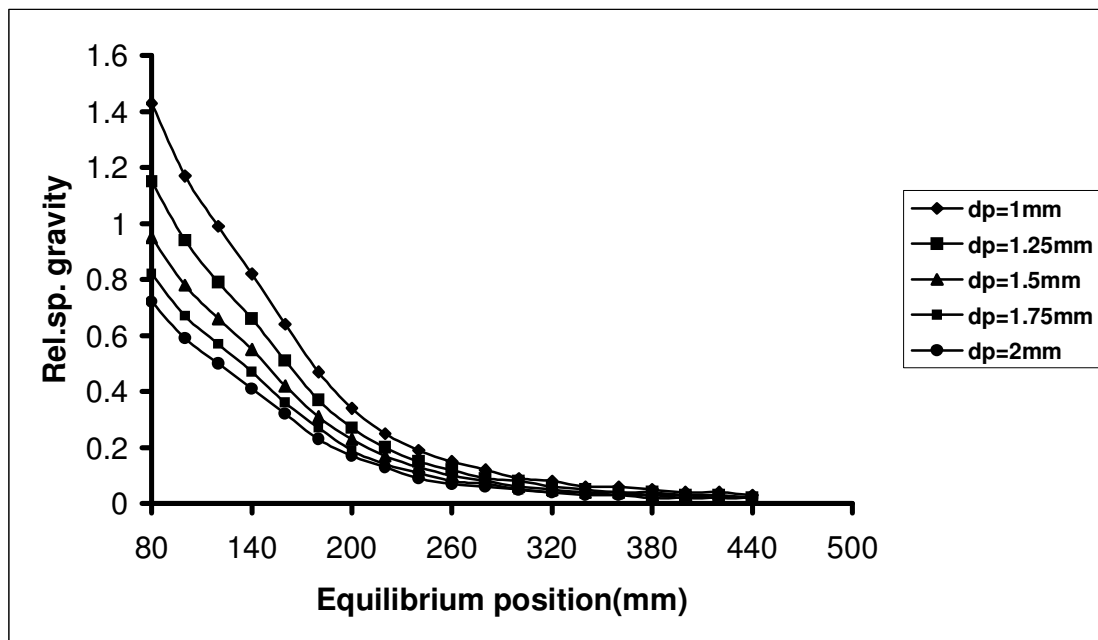


Fig.3 Effect of particle size variation on the radial distribution of relative specific gravity (feed mean flow depth =5mm)

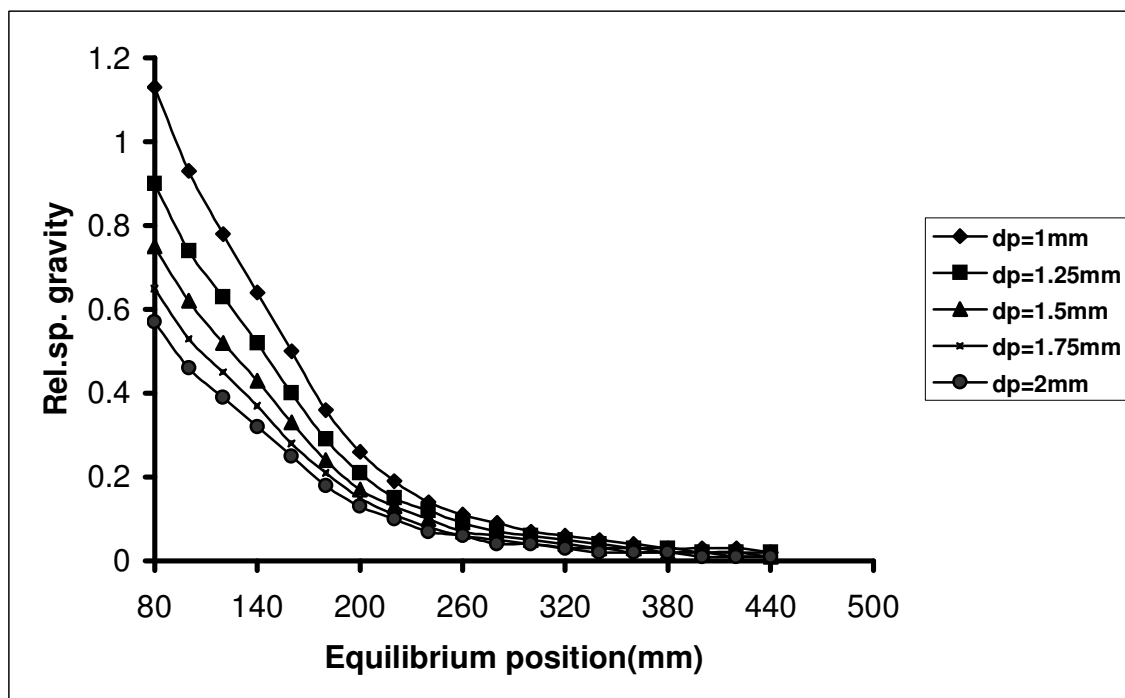


Fig.4 Effect of particle size variation on the radial distribution of relative specific gravity (feed mean flow depth =4mm)

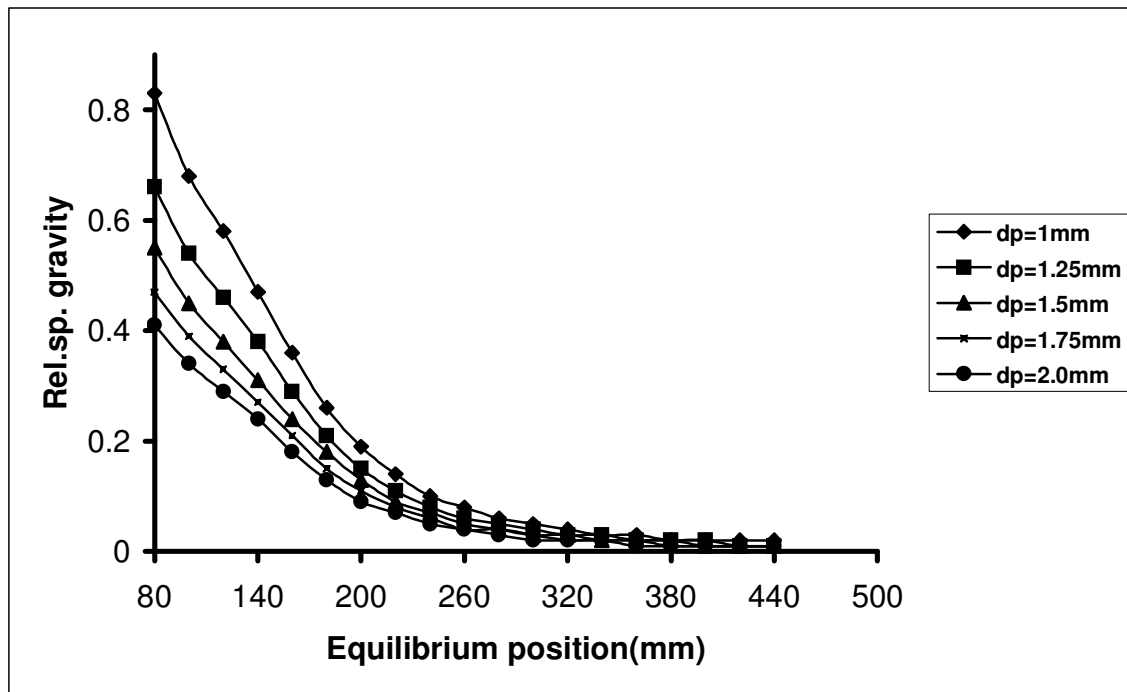


Fig.5 Effect of particle size variation on the radial distribution of relative specific gravity (feed mean flow depth =3mm)

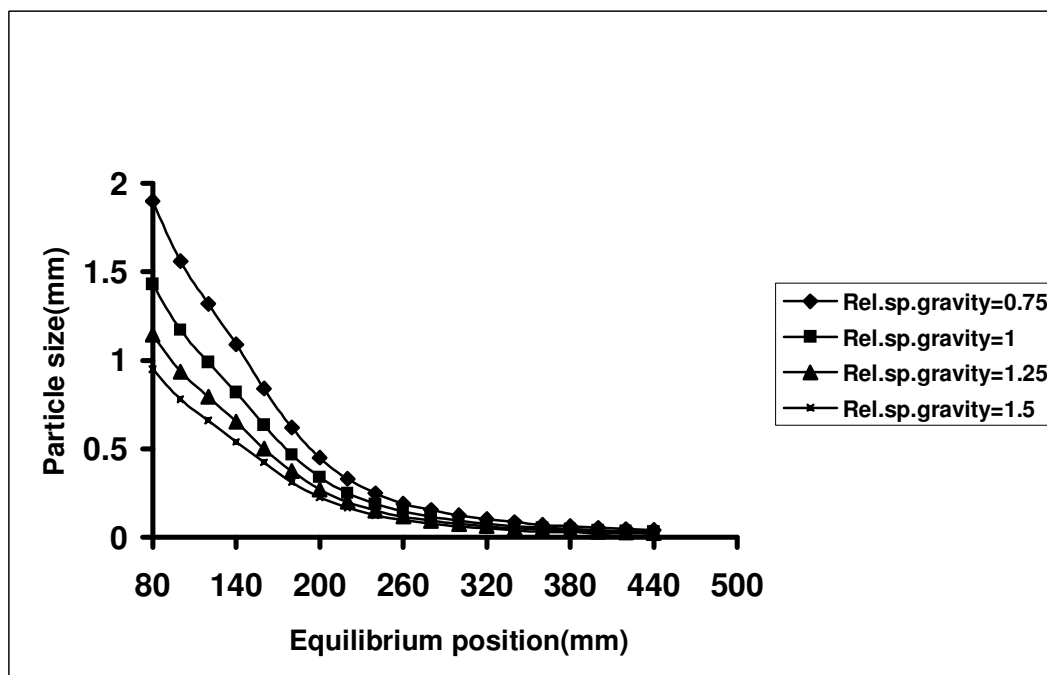


Fig.6 Effect of relative specific gravity on the radial distribution of particle size (feed mean flow depth =5mm)

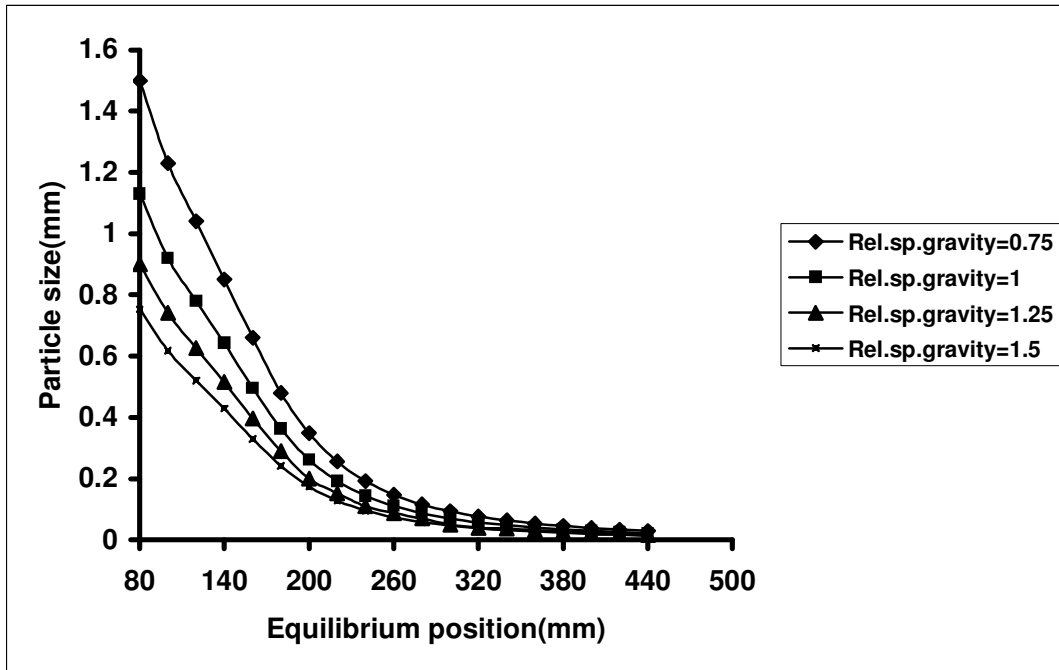


Fig.7 Effect of relative specific gravity on the radial distribution of particle size (feed mean flow depth =4mm)

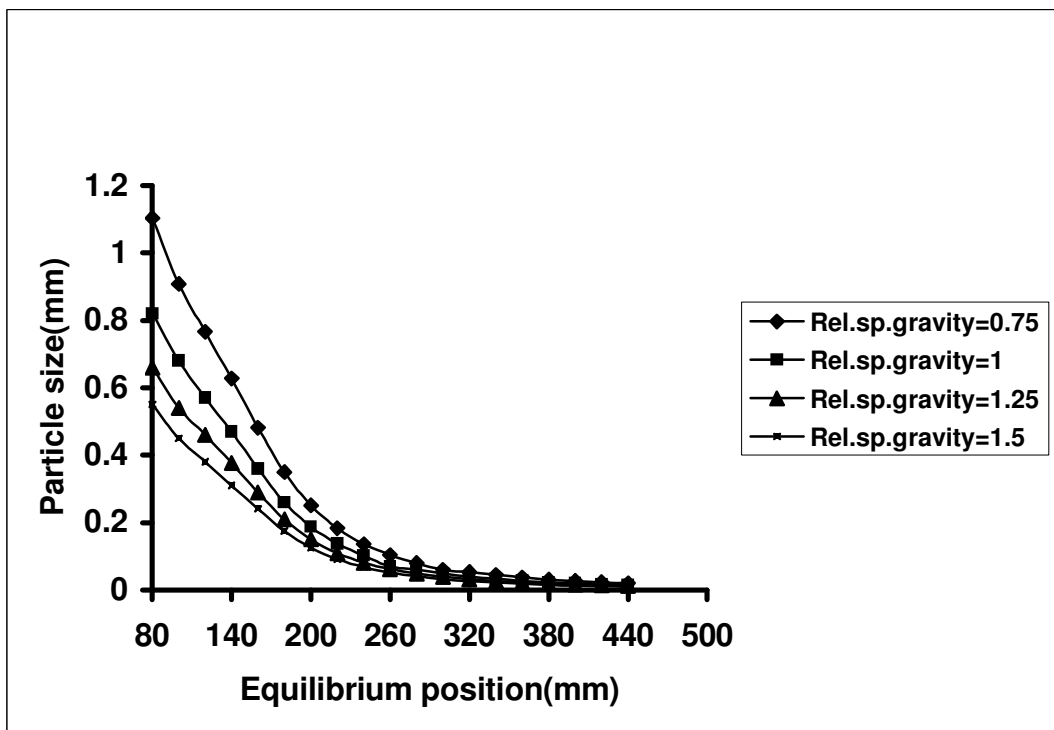


Fig.8 Effect of relative specific gravity on the radial distribution of particle size (feed mean flow depth =3mm)

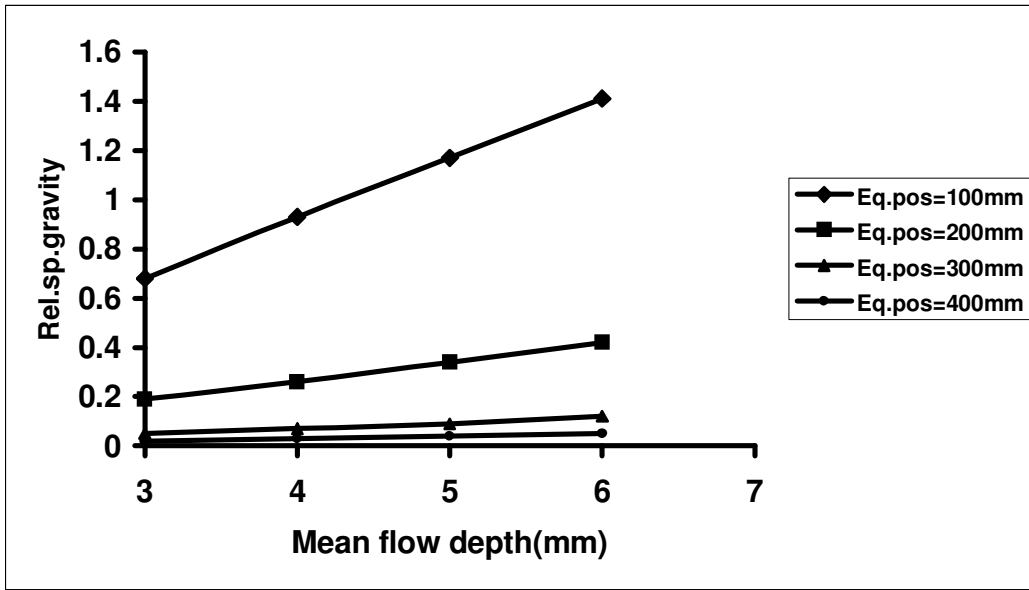


Fig.9 Sensitivity of relative specific gravity with mean flow depth at various equilibrium positions (particle size =1mm)

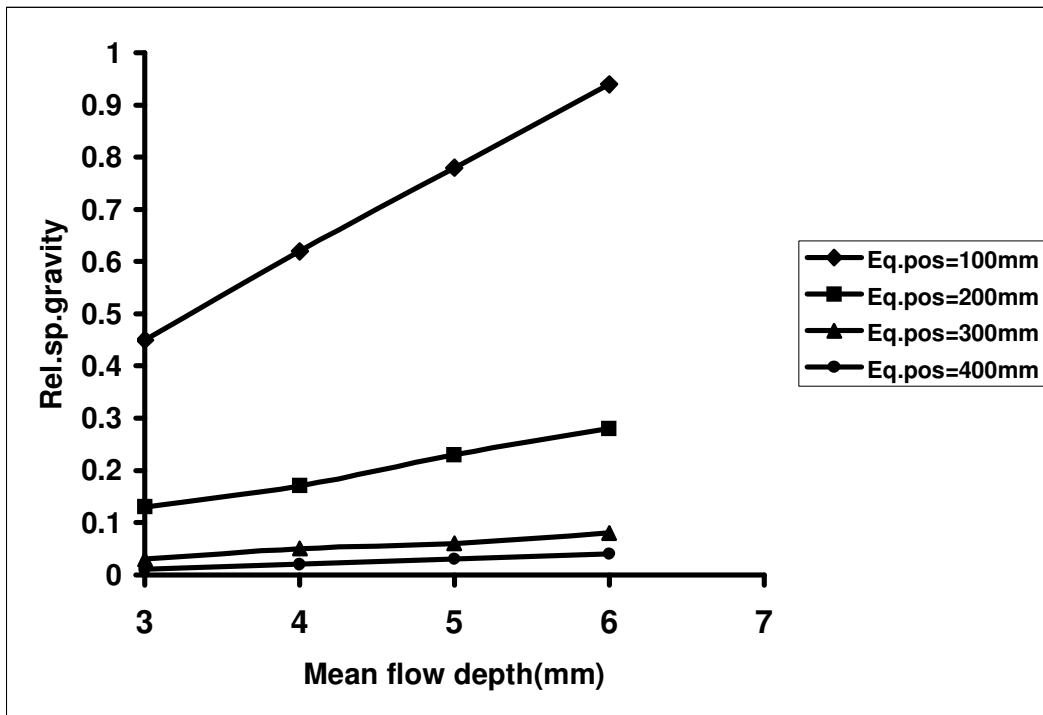


Fig.10. Sensitivity of relative specific gravity with the mean flow depth at Various equilibrium position (particle size=1.5mm)

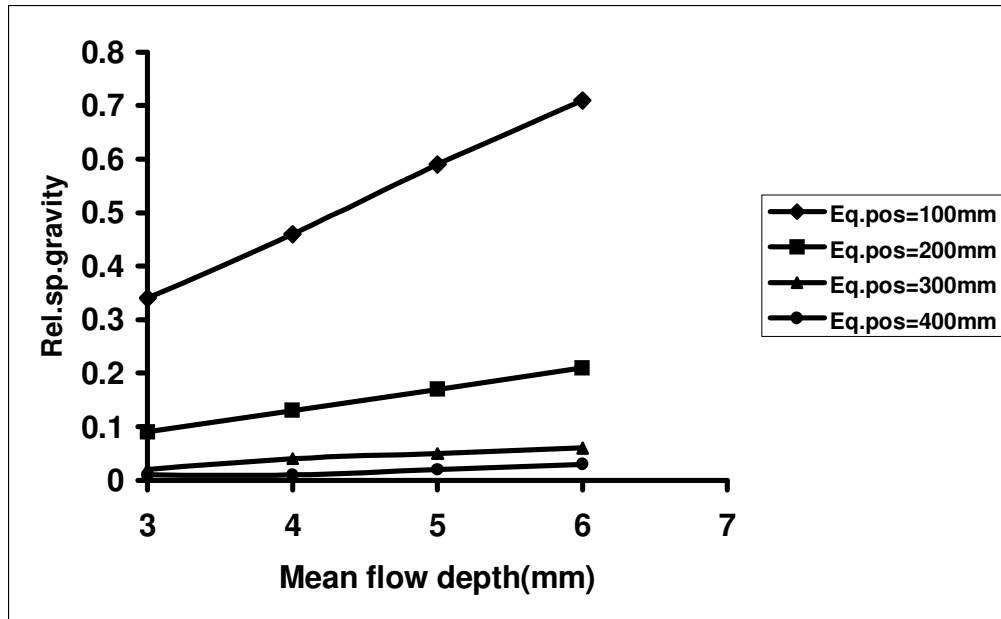


Fig.11. Sensitivity of relative specific gravity with mean flow depth at various equilibrium position (particle size =2mm)